M R S Internet Journal Nitride Semiconductor Research

Defect Trapping and Annealing for Transition Metal Implants in Group III Nitrides

K. Lorenz[1], R. Vianden[1], S.J. Pearton[2], Cammy R. Abernathy [2] and J.M. Zavada[3]
[1]*Institut fuer Strahlen- und Kernphysik der Universitaet Bonn,*
[2]*Department of Materials Science and Engineering, University of Florida,*
[3]*U.S. ARL European Research Office,*

(Received Thursday, March 16, 2000; accepted Monday, May 22, 2000)

The annealing of implantation induced lattice damage in AlN, GaN and InN was studied by means of the perturbed angular correlation (PAC) technique using the PAC probe ^{181}Hf(^{181}Ta). In all three lattices substantial fractions of the probe atoms occupied substitutional lattice sites after annealing. A detailed investigation of the changes observed during isochronal annealing indicates differences in the recovery process. In GaN the trapping of a unique defect, possibly a Nitrogen vacancy, in an intermediate temperature range was found.

1 Introduction

The group III – Nitrides AlN, GaN and InN are attractive materials for optoelectronic devices and especially GaN-based laser and light-emitting diodes are already commercialised on a large scale. However, presently available devices generally are produced by doping during growth [1] and not by ion implantation like most modern electronic devices. In order to couple such devices into integrated circuits, doping by ion implantation would be highly desirable. Besides the devices mentioned above, Er doped materials are of great interest for photonic applications such as solid state lasers, optical amplifiers, lasers storage devices and displays. The Er^{3+} intra – 4f emission at 1.54 µm corresponds to the standard wavelength used in telecommunication. Up to now Er doping of Silicon has been intensively studied, but unfortunately the luminescence efficiency is strongly quenched at room temperature. In wide band gap semiconductors like GaN this quenching is much less pronounced [2] and thus it is hoped that Er doping by implantation might open the way to fully integrated optical circuits. Thus, a profound knowledge of the annealing process, necessary to remove the implantation induced lattice damage and activate the implanted dopants, is essential. Only a few studies exist addressing this problem [3], [4] where mainly electrical properties of the dopants were measured. Here we employ the PAC technique, which delivers information on the immediate lattice surrounding of an implanted probe atom and makes it possible to follow the reconstruction of the lattice from the initial stages on. PAC requires special properties of the probe atom. Thus the probe ^{181}Hf(^{181}Ta) was employed. Since its elemental properties are similar to Rare Earths like Er, is hoped it will give information also relevant to these interesting implants. Further, due to their large band gap, the group III nitrides are very suitable for high temperature electronics. A thorough knowledge of the annealing process might also stimulate progress in this direction.

2 Experimental Details

The GaN samples used were grown by Metal Organic Chemical Vapor Deposition at 1040 °C on c-plane sapphire substrates. The layers were nominally undoped ($n \sim 5 \times 10^{16}$ cm^{-3}) and were ~3µm thick. Analysis by x-ray diffraction and transmission electron microscopy showed them to be typical of current state-of-the-art heteroepitaxial material, with rocking curve full-width-half-maximum (FWHM) of ~280 arc.sec and defect densities of ~10^9 cm^{-2} at the surface. The InN and AlN were grown by Metal Organic Molecular Beam Epitaxy at 650 and 900 °C, respectively, on c-plane sapphire. The InN was strongly n-type (~10^{19} cm^{-3}) due to the presence of native point defects and the layers were ~0.7µm thick. The x-ray FWHM was ~750 arc.sec on these layers. The AlN was resistive (>10^7Ωcm) and the layers were ~1µm thick. The x-ray FWHM was ~600 arc.sec on these samples.

https://doi.org/10.1557/S1092578300000053 Published online by Cambridge University Press

The samples were cut to 5 x 5 mm^2 pieces and without further treatment implanted at room temperature at the Bonn radioactive isotope separator with ^{181}Hf. It was produced by thermal neutron capture from the stable isotope ^{180}Hf. The implantation energy was 160 keV and typical doses reached 10^{13} at./cm^2 mainly due to stable ^{180}Hf contaminating the mass 181 line. A TRIM [5] calculation yielded ranges of 460, 314, and 333 Å for AlN, GaN and InN, respectively, and corresponding typical concentrations of ~ 4 x 10^{18} cm^{-3}.

Subsequently an isochronal annealing program was carried out in order to study the lattice damage recovery. The annealing steps were performed in a Rapid Thermal Annealing apparatus [6] between graphite strips under a Nitrogen atmosphere at ambient pressure. Additionally, a second, un-implanted piece of GaN was placed on the sample as a proximity cap to protect the surface. Typical holding times were 120 s and maximum temperatures of 1773 K were reached in the case of AlN.

Prior to the start of the programme and after each annealing step a PAC spectrum was taken with 4 detectors (equipped with BaF_2 scintillators) set up in a plane in a cross shaped arrangement. The PAC technique exploits the fact that in suitable nuclei an excited nuclear state is reached through the decay of a parent isotope and with a characteristic half life, $t_{1/2}$ = 10.8 ns in the case of ^{181}Hf(^{181}Ta), decays by the emission of a second nuclear radiation. Due to the law of conservation of angular momentum, the directions of emission of the populating and depopulating radiation in this so-called γ-γ cascade are correlated. In the absence of hyperfine fields at the site of the probe nucleus this correlation remains constant in time. Changes of the directional correlation of the two γ rays indicate, that during the lifetime of the intermediate state a hyperfine interaction between the quadrupole moment of the nucleus and an electric field gradient (EFG) has taken place. A PAC spectrum is extracted from the coincidence count rate N(t) recorded for pairs of detectors, where t is the time elapsed between the detection of the first and the second γ ray. In the case of pure electric quadrupole interaction, like it is expected in the non-cubic semiconductors studied here, N(t) has the following form:

$$N(t) \approx e^{-\frac{\ln 2 \cdot t}{t_{1/2}}} \cdot \sum_{n=0}^{n_{max}} s_n(\alpha_i, \eta) \cdot \cos\left[c_n(\eta) \cdot \nu_Q \cdot t\right] \cdot e^{-\delta \cdot c_n(\eta) \cdot \nu_Q \cdot t} \quad (1)$$

The leading exponential factor contains only the nuclear half life $t_{1/2}$ and can be eliminated. The second factor, the perturbation function, is responsible for the modulation of a PAC spectrum. After a fit to the data it is possible to extract the parameters of the quadrupole interaction from it. The magnitude of the interaction is described by the quadrupole interaction constant:

$$\nu_Q = \frac{e \cdot Q \cdot V_{zz}}{h}. \quad (2)$$

Apart from the elementary charge e and Planck´s constant h, ν_Q is given by the product of the nuclear quadrupole moment Q and V_{zz}, the principal component of the EFG tensor at the nuclear site. The quadrupole moment Q of the intermediate 5/2 state of the 133 – 482 keV γ-γ cascade in ^{181}Ta has a value of Q(5/2)=(+)2.36(5) b [7]. Therefore, the magnitude of the EFG can be derived directly from ν_Q. Further, the PAC spectrum is sensitive to the symmetry of the electric field gradient tensor, described by the asymmetry parameter η, which influences the frequency factors $c_n(\eta)$ and the coefficients $s_n(\alpha_i, \eta)$ and consequently can also be determined. Finally, if the measurement is carried out in a single crystal, it is possible to extract the orientation of V_{zz} relative to the crystal axes from the Euler angles contained in the $s_n(\alpha_i, \eta)$ coefficients. The second exponential term with the additional parameter δ allows for a Lorentzian distribution of interaction frequencies around ν_Q . Most of the following measurements were carried out in a geometry where the ⟨0001⟩-axis of the Wurtzite lattice is aligned with the angle bisector of two detectors under 90°. Further details of the application of the PAC technique to the study of solid state properties and the data reduction procedure can be found elsewhere [8].

Internal fields at the site of probe nuclei in solids are dominated by contributions from charges and spins within the first few atomic shells. More distant charges and spins only contribute to an inhomogeneous broadening of the signals from these nearby few shells, manifesting itself in an increase of the damping parameter δ. As a result, hyperfine interaction frequencies measured by PAC characterise the different local atomic environments in which the probe atoms find themselves. Thus, PAC can be used as a tool to study the structure and changes of local environments after different treatments of a sample. Isochronal annealing programmes, where the sample is annealed at increasingly higher temperatures T_A with intermediate measurements at the base temperature, here 293 K, have been proven to be particularly successful to follow the reconstruction of a lattice after being damaged, for instance, by implantation. Further, the onset of migration of a given defect interacting

https://doi.org/10.1557/S1092578300000053 Published online by Cambridge University Press

with a probe atom can be observed or the binding energy of a probe atom - defect pair can be determined.

3 Results and Discussion

After the implantation, prior to any annealing, a damped oscillation was observed in the PAC spectra for GaN and InN (Figs. 1a, 4a). This indicates that at the end of the collision cascade a small fraction f_s of the implanted probe atoms stops on well defined lattice sites. Least squares fits [9] to the data yield values for f_s of 36% for GaN and 19% for InN. These relatively high values for f_s as compared to AlN can be ascribed to the higher replacement collision probability due to the larger mass of the group III atom. However, following this argument one would expect an even higher fs in InN than in GaN. The fact that with 19%, fs in InN is only about half the value for GaN is most probably due to the lower crystal quality of the InN material, which also leads to a lower final substitutional fraction after annealing (see discussion below). In all three cases the width of the frequency distribution δ is quite large, 20(1) % in GaN and 10(1) % in InN. The following annealing process for the three compounds showed quite different features so that in the following it will be described separately for GaN, InN, and finally AlN.

3.1 GaN

Immediately after implantation most (64%) of the implanted ^{181}Hf probes are situated in a lattice environment strongly disturbed by the implantation induced damage. They cause the sharp drop of the anisotropy in the first few nanoseconds in figure 1a and are characterised by a broad distribution of quadrupole interaction frequencies around 1000 MHz. However, in the same spectrum already a faint modulation can be observed. It is due to a fraction f_s = 36% of the implanted probes, which occupy less disturbed lattice sites with a quadrupole interaction frequency of ν_{Q1} = 332(2) MHz (δ_1 = 21 %, η_1 = 0). Then, annealing causes an interesting development. First, up to a temperature of T_A = 673 K, the damping parameter δ drops from 21 % to 11% without a strong change in f_s (see Figure 2). Subsequently δ continues to decrease, although more slowly, whereas the fraction of probes on regular lattice sites starts to grow steadily until at T_A = 1373 K typically values of f_s = 70% to 80% are reached. After the annealing step at 1373 K a quadrupole interaction constant of ν_{Q1} = 338(2) MHz (δ_1 = 3%, η_1 = 0) was derived.

The orientation of the corresponding EFG was checked by taking not only spectra with the sample's ⟨0001⟩-axis oriented in the standard direction (Figure 3a) as described above, but also with the ⟨0001⟩-axis perpendicular to the detector plane (Figure 3b) or pointing towards one detector (Figure 3c). The results, a doubling of the period in the first case and a practically vanishing oscillation in the second, are in perfect agreement with the assumption that V_{zz}, the principal component of the EFG, is oriented parallel to the ⟨0001⟩-axis of the Wurtzite structure. The small contribution of the second and first harmonic in figure 3 b and c can be explained by a slight deviation from the perfect orientation.

Since GaN crystallises in the hexagonal Wurtzite structure an axially symmetric EFG with its principal component oriented along the ⟨0001⟩-axis is expected at a regular lattice site. Thus, the observation of a unique EFG with this orientation indicates that the corresponding fraction f_S of probe nuclei occupies regular sites. Due to the large difference in the covalent radii of Hf (r_C=1.44 Å) and N (r_C=0.75 Å) the incorporation of Hf on N sites is very improbable and the incorporation on Ga sites (r_C= 1.26 Å) is more likely. This was confirmed by recent RBS measurements, which show that implanted Hf fully replaces Ga in GaN [10].

Dividing the measured QIF by the quadrupole moment Q = 2.36 b [7] of the 5/2 intermediate state of the γ-γ cascade in ^{181}Ta and the Sternheimer antishielding factor (1-γ_∞) = 62 [11] of the Ta ion the lattice EFG at the Ga site can be calculated to be V^{zzlatt}=0.96 x 10^{16} V/cm^2. This agrees well with the value of V^{zzlatt}=0.65 x 10^{16} V/cm^2 derived in the same way from NMR measurements for Ga in GaN [12], further confirming the complete substitutionality of the Hf probe.

At low annealing temperatures a second quadrupole interaction frequency ν_{Q2} = 1378(9) MHz with an asymmetry parameter η_2 = 0.63(2) is necessary to describe the spectra. A fraction of f_D = 25% of the probe atoms is subjected to the corresponding EFG (Figure 2a). Immediately after implantation this EFG is highly non-unique resulting in large frequency distribution parameter δ_2 = 23 %, but $\delta_2$drops parallel to δ_1 (Figure 2b) and after annealing at 773 K the frequency is clearly visible in the PAC spectrum (Figure 1b). The fraction f_D reaches a maximum of 28% at 573 K and disappears after annealing above 1000 K (Figure 2b). The large value of ν_{Q2} is characteristic for a deviation from the regular lattice structure in the nearest neighbourhood of the probe atoms. The low value of δ_2 implies that this deviation has a regular structure, i.e. does not correspond to an amorphous environment. Similar situations have been observed in other semiconductors and are indicative of a unique defect trapped at the probe atom [13]. Since no diffusion in the Ga sub-lattice is expected in GaN below 1273 K [14], and the defect – probe atom

https://doi.org/10.1557/S1092578300000053 Published online by Cambridge University Press

complex breaks up below 1000 K, we suggest that a Nitrogen vacancy, trapped at the slightly oversized Hf probes, causes the corresponding quadrupole interaction. Estimates for a nearest neighbour vacancy in the point charge model [15] yield a magnitude of the observed EFG which is in good agreement with the experimental value. However, it seriously underestimates the lattice EFG at the Ga site and therefore cannot explain the large asymmetry parameter η_2.

Summarising, the PAC data lead to the following picture of the annealing process. For a fraction corresponding to the initial f_S after the implantation no defect remains in the immediate vicinity of the probe atom. Thus the lattice EFG is only slightly disturbed by more distant defects leading to the observed frequency distribution. Annealing leads to a partial recovery of these defects thus narrowing δ_1. Due to the larger mobility of Nitrogen - Nitrogen loss has been observed well below 1273 K [14] - these are most probably defects of the Nitrogen sub-lattice. For the remaining fraction, defects in the nearest neighbourhood seriously disturb the lattice EFG. It takes temperatures well above 1000 K, where also diffusion in the Ga sub-lattice sets in, to restore the surrounding lattice leading to a unique EFG at over 80% of the Hf probe sites. A small fraction of probes traps a Nitrogen vacancy at a nearest neighbour site. The corresponding quadrupole interaction frequency also narrows until at 1000 K complete de-trapping occurs and the substitutional fraction is increased. Assuming in a simple model, that the de-trapping is a one step process, a binding energy $E_B \cong 3$ eV can be estimated. Here a Debye temperature of 586 K was used [16].

3.2 InN

Directly after the implantation a fraction f_S = 19 % of the implanted ^{181}Hf probes show a well defined quadrupole interaction frequency of ν_{Q1} = 668(5) MHz (δ_1 = 13%, η_1 = 0) (Figure 4a). Annealing causes a continuous increase of this fraction, until, after the 1173 K step, 43 % of the probes occupy regular lattice sites (Figure 5a). δ drops rapidly to 3.5 % at 1173 K (Figure 5b). A final value for ν_{Q1} = 666(1) MHz (δ_1 = 3.5 %, η_1 = 0) is reached. An orientation measurement yielded the same orientation of the electric field gradients principal axis as in GaN, i.e. parallel to the c axis.

The data suggest that like in GaN a small fraction f_S of the implanted probes comes to rest on substitutional In sites at the end of the collision cascade. However, the lower value of δ is indicative of less severe implantation damage in this case. Unlike in GaN, here annealing causes a steady increase of f_S up to 44%, whereas δ remains essentially constant up to 600 K before it drops to its final value at 1200 K. The maximum of 43% of Hf incorporated into an undisturbed InN lattice is only about half the value reached in GaN. This can be either due to the lower crystal quality of the InN sample (due to the higher lattice-mismatch with sapphire) or to the not yet optimised annealing procedure and will be subject of further investigations. No evidence for the trapping of a was found in this lattice. Since the covalent radii of Hf and In are equal (r_C=1.44 Å), this can be explained by the lack of any attractive strain introduced by the Hf probe.

3.3 AlN

Directly after the implantation all probe atoms come to rest in a highly damaged lattice environment resulting in a strong damping of the PAC spectrum (Figure 6a). This can be described by a broad quadrupole frequency distribution around ν_{Q1} = 922(11) MHz (δ_1 = 40%). Annealing leaves the spectrum unchanged until at 773 K a second, much narrower, frequency distribution (ν_{Q2} = 323(10) MHz, η_2 = 0, δ_2 = 9%) appears in the spectrum (Figure 6b). Its fraction fs increases only slightly to 13% at 1173 K and then decreases again (Figure 7). The damping parameter δ_2 remains virtually constant in the temperature range investigated, indicating that no further annealing of the implantation damage occurs. Considering the high melting point T_M = 3273 K of AlN and the fact that lattice damage recovery stages are usually correlated to it, the temperature where ν_{Q2} appears is quite low. So the frequency is probably due to the annealing of correlated damage, i.e. Hf probes moving into Al vacancies which remained in their vicinity at the end of the collision cascade. The highest annealing temperatures reached in this study correspond to only about half the melting point, a temperature where in GaN the incorporation of Hf onto Ga sites only starts. Therefore in the case of AlN much higher temperatures seem necessary to restore the lattice order. Such annealing seem feasible since no signs of lattice destruction due to the out - diffusion of N (or decomposition of the surface) was observed up to the highest annealing temperature.

Measurements for different orientations of the sample did not show significant differences, which due to a near polycrystalline structure of the AlN films, is not surprising.

From the quadrupole interaction frequencies the following values of the electric field gradients for the Hf probe on a group III lattice site can be derived as described above: GaN 9.5(2) x 10^{15} V/cm^2, InN 18.9(3) x 10^{15} V/cm^2 and AlN 9.2(2) x 10^{15} V/cm^2 . Estimates in the point charge model mentioned above [15] yield values of 0.27, 0.43 and 1.56 x 10^{15} V/cm^2, respectively. Here lattice constants given by Nakamura and

https://doi.org/10.1557/S1092578300000053 Published online by Cambridge University Press

Fasol [17] and a charge of Z = +1 for the cation and –1 for N were used. Assuming first order exponential kinetics and de-trapping of the vacancy in a one step dissociation process, a binding energy of $E_B \sim 3$ eV can be estimated. However, it is probable that the bad agreement is not only due to the known inadequacies of this model but also to uncertainties in the crystallographic data [16], mainly the so called u parameter.

4 Conclusions

Implantation of ^{181}Hf into GaN, AlN and InN was studied by PAC. After implantation, substitutional fractions of 36% for GaN, 19% for InN and 0% for AlN were found. Subsequent annealing increased these values to ~80% for GaN, 43% for InN and 12% for AlN. The PAC data provides strong evidence for the role of defect reactions in controlling the recovery of implantation damage in the group III-nitrides.

ACKNOWLEDGMENTS

We gratefully acknowledge partial support of this work by the BMBF (03-MA5BON). The work at UF is partially supported by NSF-DMR 972865 and by the Army Research Office. The support of the GKSS-Forschungszentrum Geesthacht GmbH, Max-Planck-Straße, 21502 Geesthacht is gratefully acknowledged

REFERENCES

[1] S. Nakamura, T. Mukai, M. Senoh, *Jpn. J. Appl. Phys.* ***30***, L1998 (1991).

[2] U. Hommerich, M. Thaik, RN. Schwartz, RG. Wilson, JM. Zavada, SJ. Pearton, CR. Abernathy, JD. MacKenzie, Proc. of the Symp. on Light Emitting Devices for Optoelectronic Applications and Twenty-Eighth State-of-the-Art Program on Compound Semiconductors. Electrochem. Soc. 1998, pp.110-18. Pennington, NJ, USA

[3] X.A. Cao, S.J. Pearton, R.K. Singh, C.R. Abernathy, J. Han, R.J. Shul, D.J. Rieger, J.C. Zolper, R.G. Wilson, M. Fu, J.A. Sekhar, H.J. Guo, S.J. Pennycook, *MRS Internet J. Nitride Semicond. Res.* ***4S1***, G6.33 (1999).

[4] HH Tan, JS Williams, J Zou, DJH Cockayne, SJ Pearton, RA Stall, *Appl. Phys. Lett.* ***69***, 2364-2366 (1996).

[5] J. P. Biersack, L. G. Haggmark, *Nucl. Instrum. Methods B* ***174***, 257 (1980).

[6] S. S. Gill, B. J. Sealy, *J. Electrochem. Soc.* ***133***, 2590 (1986).

[7] T. Butz, A. Lerf, *Phys. Lett.* ***97A***, 217 (1983).

[8] G. Schatz, A.Weidinger, JA. Gardner, "Nuclear Condensed Matter Physics (Nuclear Methods and Applications)" John Wiley & Sons, (1996) Chichester, New York, Brisbane, Toronto, Singapore

[9] N. P. Barradas, M. Rots, A. A. Melo, J. C. Soares, *Phys. Rev. B* ***47***, 8763 (1993).

[10] E Alves, MF da Silva, JG Marques, JC Soares, K Freitag, *Mater. Sci. Eng. B* ***59***, 207-210 (1999).

[11] F. D. Feiock, W. R. Johnson, *Phys. Rev.* ***187***, 39 (1969).

[12] G. Denninger, D. Reiser, *Phys. Rev. B* ***55***, 5073 (1997).

[13] "Characterization of defect structures by perturbed angular correlation technique",T. Wichert, Characterization of Defects in Materials Symposium. Mater. Res. Soc. 1987, pp.35-51

[14] S. Strite, A. Pelzmann, T. Suski, M. Leszczynski, J. Jun, A. Rockett, Markus Kamp , K. J. Ebeling, *MRS Internet J. Nitride Semicond. Res.* ***2***, 15 (1997).

[15] F. DeWette, *Phys. Rev.* ***123***, 103 (1961).

[16] X. L. Chen, J. K. Liang, Y. P. Xu, P. Z. Jiang, Y. D. Yu, K. Q. Lu, Mod, *Phys. Lett. B* ***13***, 285 (1999).

[17] Shuji Nakamura, Gerhard Fasol, *The Blue Laser Diode - GaN based Light Emitters and Lasers* , (Springer-Verlag, Heidelberg, 1997), .

FIGURES

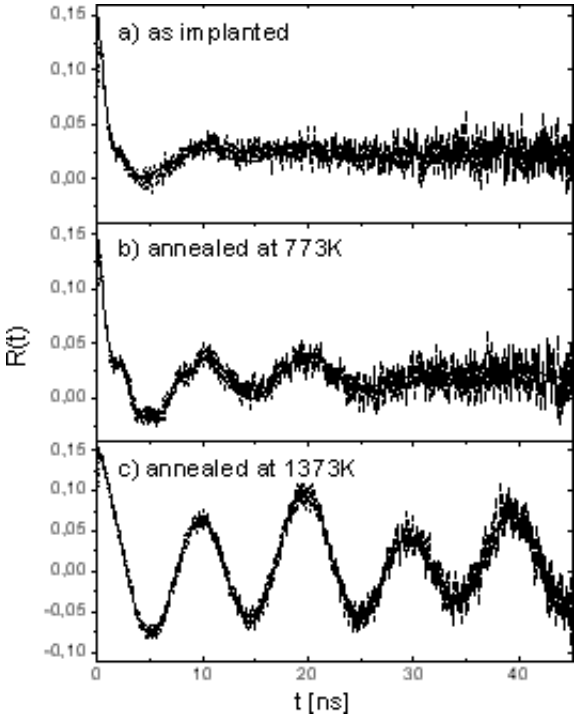

Figure 1. Time dependent anisotropy observed for ^{181}Hf in Wurtzite GaN after implantation and RTA annealing for 120 s at temperatures indicated in the frames. The <0001> axis was aligned with the angle bisector between two detectors under 90°. The solid lines represent least squares fits to the data.

https://doi.org/10.1557/S1092578300000053 Published online by Cambridge University Press

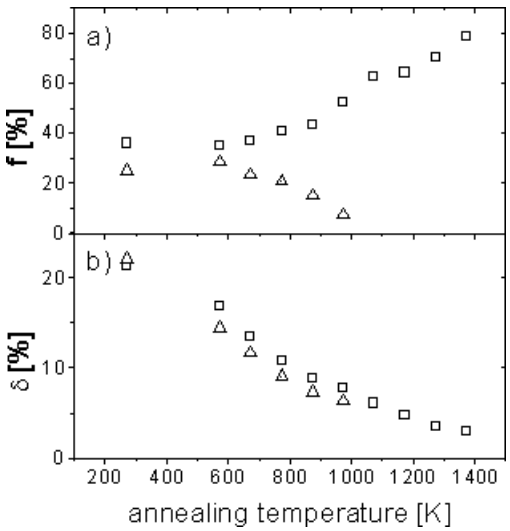

Figure 2. (a) Fraction of ^{181}Hf probes in GaN showing the unique quadrupole interaction of ν_{Q1} = 338 MHz (open squares) after various steps of isochronal annealing programmes and the fraction associated with a defect (open triangles). (b) Width δ of the frequency distribution around ν_{Q1} (open squares) and ν_{Q2} (open triangles).

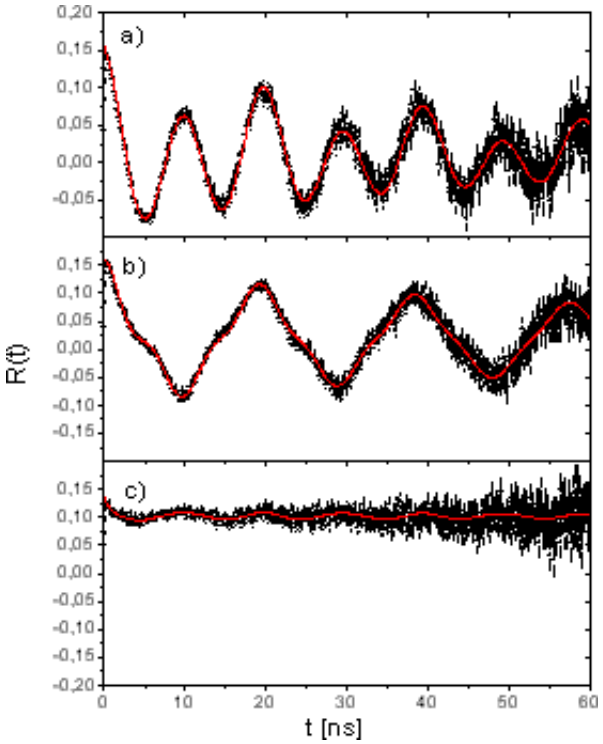

Figure 3. Time dependent anisotropy observed for ^{181}Hf in Wurtzite GaN after annealing for different orientations of the <0001> axis. a) aligned with the angle bisector between two detectors under 90°, b) perpendicular to the detector plane, c) aligned with one detector axis. The solid lines represent least squares fits to the data.

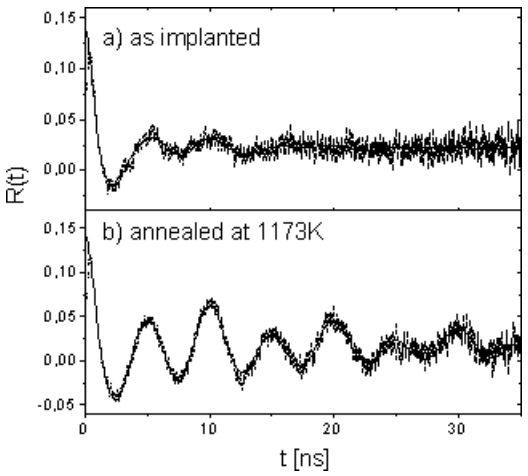

Figure 4. Time dependent anisotropy observed for ^{181}Hf in Wurtzite InN (for details see figure 1)

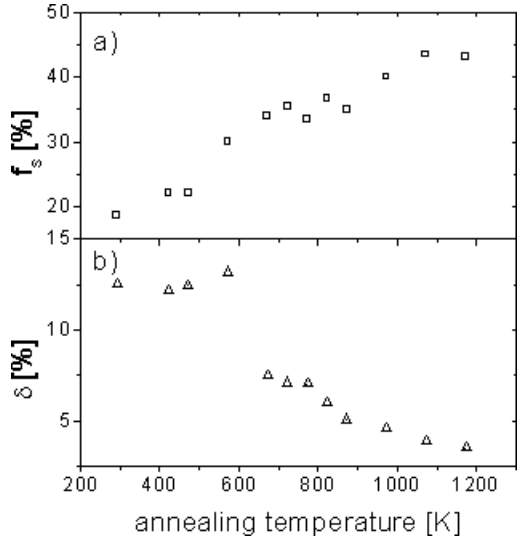

Figure 5. (a) Fraction f_D of ^{181}Hf probes in InN showing the unique quadrupole interaction of ν_Q = 666 MHz after various steps of an isochronal annealing programme, (b) Width δ of the frequency distribution around ν_Q.

https://doi.org/10.1557/S1092578300000053 Published online by Cambridge University Press

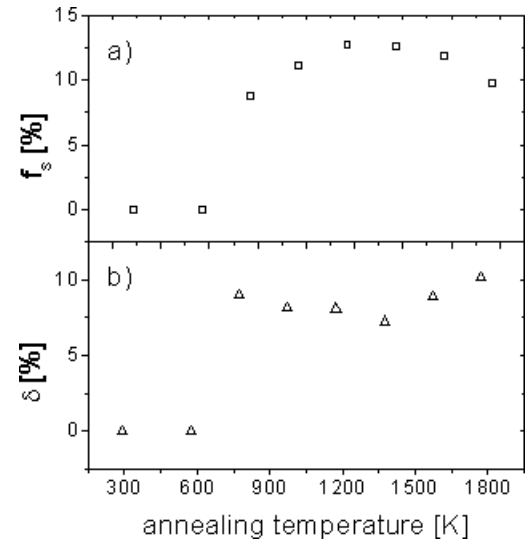

Figure 6. Time dependent anisotropy observed for ^{181}Hf in Wurtzite AlN (for details see figure 1)

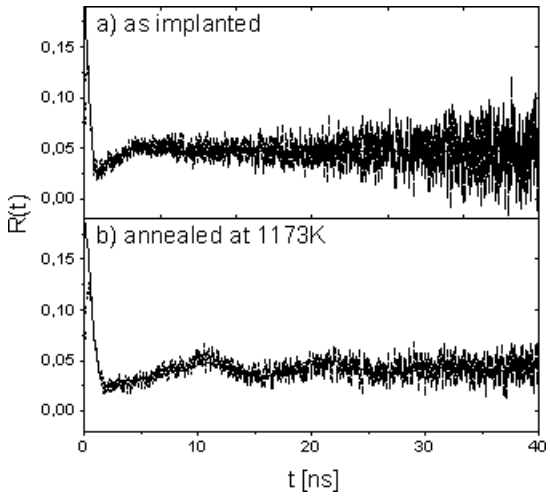

Figure 7. (a) Fraction f_D of ^{181}Hf probes in AlN showing the unique quadrupole interaction of ν_Q = 323 MHz after various steps of an isochronal annealing programme, (b) Width δ of the frequency distribution around ν_Q.

https://doi.org/10.1557/S1092578300000053 Published online by Cambridge University Press